

Picosecond Laser Photolysis Studies on Chain-Length, Solvent and Temperature Dependences of the Intramolecular Photoreduction Process of Benzophenone by Diphenylamine

Hiroshi Miyasaka,^{*, #} Manabu Kiri, Kazuhiro Morita, Noboru Mataga,^{*, ##} and Yoshifumi Tanimoto[†]

Department of Chemistry, Faculty of Engineering Science, Osaka University, Toyonaka, Osaka 560

[†]Department of Chemistry, Faculty of Science, Hiroshima University, Kagamiyama, Higashi-Hiroshima 724

(Received December 7, 1994)

Photoinduced hydrogen abstraction (HA) processes of 1-(4-anilinophenyl)-2-(4-benzophenoxy)ethane, 1-(4-anilinophenyl)-3-(4-benzophenoxy)propane, and 1-(4-anilinophenyl)-8-(4-benzophenoxy)octane (BP-O-(CH₂)_n-O-DPA: *n*=2, 3, and 8) in benzene, acetonitrile, and *N,N*-dimethylformamide solutions were investigated by means of picosecond transient absorption spectroscopy. In benzene solution, apparent mechanism of the hydrogen abstraction reaction was "direct" process and no absorption spectrum of the charge separated state was observed. The decay of triplet benzophenone moiety (³BP*) was regulated by the dynamic rearrangement process of the mutual geometry between ³BP* and DPA to a more compact one.

In polar solutions, the electron transfer (ET) from DPA to ³BP* moiety took place in addition to the direct HA from DPA by ³BP*. The rate of the ET reaction was regulated mainly by the distance between the reactant moieties. Moreover, the intra-ion pair (IP) proton transfer (PT) resulting in the HA product formation was observed, although such PT process in the IP state between the unlinked ³BP* and the *secondary* amine was not observed. By integrating the present results on the linked systems with those of the unlinked systems, the role of the ET or CT interaction in the HA process of ³BP* from the *secondary* amine was discussed.

Electron transfer (ET) and related processes play fundamental roles of crucial importance in many photochemical reactions taking place in condensed phase and a number of experimental as well as theoretical investigations have been performed from various viewpoints.^{1–6)} Hydrogen abstraction reaction of excited benzophenone (BP*) from aliphatic and aromatic amines (AH) in solutions is one of the most typical reactions closely related to these fundamental processes.^{7–22)} In general, BP* abstracts hydrogen from various kinds of compounds, among which the yields of the reaction with amines are very high and the rate constants are close to the diffusion-controlled ones. On the basis of these experimental results, it was proposed that the stable ion pair (IP) and/or charge transfer (CT) state between BP* and AH, BP*...AH⁺, participate as an important intermediate species in the hydrogen abstraction.⁹⁾

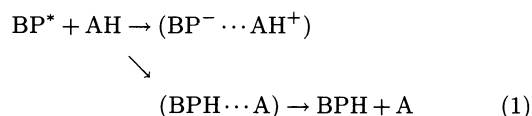
[#]Present address: Department of Polymer Engineering and Science, Kyoto Institute of Technology, Matsugasaki, Sakyo-ku, Kyoto 606.

^{##}Present address: Institute for Laser Technology, Utsubo-Hommachi 1-8-4, Nishi-ku, Osaka 550.

The elucidation of the role of ET and/or CT interactions in the hydrogen abstraction of BP*, which is the main object of the present work, may also provide significant information on the ET mechanism itself as pointed out in the following. In general, proton transfer (PT) and hydrogen atom transfer processes are much more sensitive to the mutual geometry such as the intermolecular distance and orientations of donor (D) and acceptor (A) than the ET reactions. Hence, the PT process in the IP state produced by the ET and/or the hydrogen abstraction reaction with the aid of the CT interaction may be strongly affected by the structure of the intermediate transient charge separated states. Accordingly, investigations on these reactions could provide conversely the structural information on the transient charge separated state, its relation to the energy gap for the charge separation (CS) and the mode of the IP formation ET at encounter or by excitation of the ground state CT complex, and so on. Along this line, we have been performing hitherto picosecond and femtosecond laser photolysis studies on the photoreduction processes of BP by amines as follows.^{15–22)}

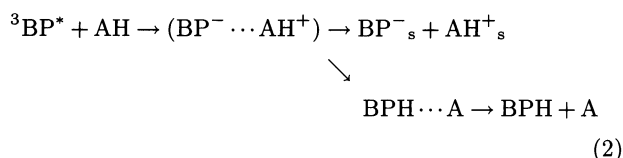
It was revealed^{15,16,22)} that the reaction mechanism

on the hydrogen abstraction of triplet BP* (³BP*) from secondary amines such as diphenylamine in various kinds of solutions at room temperature was represented by the following scheme.



where BP[−] and BPH are anion and ketyl radicals of BP, and AH⁺ and A are the cation and the hydrogen-abstracted neutral radicals of AH, respectively. That is, the hydrogen abstraction reaction and the stable IP and/or CT state formations compete with each other at encounter collision. In addition, the PT process in the stable IP produced by the ET between BP* and AH does not occur and only the ionic dissociation was observed in polar solutions.

On the other hand, the mechanism of the hydrogen abstraction from tertiary aromatic amines in strongly polar solutions such as acetonitrile was given by,



where intra-IP PT process took place in competition with the ionic dissociation terminating in free ions (BP[−]_s and AH⁺_s).^{17,19–21} In addition, it was confirmed that intra-IP PT rate was strongly dependent on the energy gap for CS, $-\Delta G_{\text{CS}}$: with increase of $-\Delta G_{\text{CS}}$, the PT rate dramatically decreased together with the slight increase of the rate constant of the ionic dissociation. These results indicated that the CS process took place at longer encounter distance for larger $-\Delta G_{\text{CS}}$, leading to the decrease of the intra-IP PT rate and increase of the ionic dissociation rate.^{19–21} It should be pointed out here that, for the reasonable interpretations on the energy gap dependence of the CS reaction between the excited and quencher molecules at encounter, it is necessary in general to take into account the donor–acceptor distance distribution and the dependence of the average distance upon $-\Delta G_{\text{CS}}$, as demonstrated by detailed theoretical investigations recently.^{23–25}

Since the intersystem crossing time constant of excited singlet state of BP, ¹BP*, is very short (ca. 10 ps), studies on the photochemistry of BP has been focused on the reactions of ³BP*. However, in the concentrated solutions of AH as usually employed for the picosecond laser photolysis studies, CS between ¹BP* and AH as well as the excitation of the weak CT complex between BP and AH formed in the ground state, which also results in the production of IP state, are not negligible. From detailed investigations on the reaction mechanisms of each IP,^{19–21} it was revealed that the

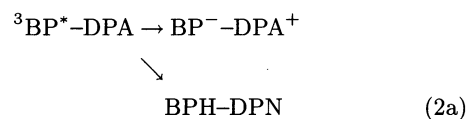
mode of the production of IP also strongly affected the subsequent PT rates even if the same AH was used as hydrogen donor. That is, the IP produced by the ET between ³BP* and AH, IP formed by ET between ¹BP* and AH, and IP via the excitation of the ground state CT complex show dynamic behaviors quite different from each other. These experimental results strongly indicate that the mutual geometry between the excited BP and AH at the CS plays a crucial role in the subsequent processes.

On the basis of these findings, we have reconsidered the difference in the apparent reaction mechanism depending on the structure of amines. Although the apparent mechanism is the “direct” hydrogen abstraction (HA) process for the reaction of BP* with secondary as well as primary amines, CT or ET interaction seems to play an important role in the HA process at encounter since the HA reaction yield and the rate constant are much larger in the reaction with primary and secondary AH than those with other compounds such as 2-propanol.

In order to elucidate more details of the role of the ET or CT interaction in the HA of BP* from secondary amines, we have performed picosecond laser photolysis studies on the intramolecular reaction process in acetonitrile solutions of BP and AH linked by spacers, where the mutual geometry between BP and AH is restricted both in the ground state static configuration and in the course of dynamic process in the excited state. The observed results of photoinduced HA processes of 1-(4-anilinophenyl)-3-(4-benzophenoxy)propane (BP–O–(CH₂)₃–O–DPA: BO3OD) and 1-(4-anilinophenyl)-2-(4-benzophenoxy)ethane (BP–O–(CH₂)₂–O–DPA: BO2OD) in acetonitrile solution²² revealed that almost all BPH production was via the PT in the IP state formed by the photoinduced ET in the case of BO2OD, as represented by the following consecutive Scheme 1a.



where – represents the spacer, –O–(CH₂)_n–O–, and DPN is the hydrogen-abstracted neutral radical of DPA. On the other hand, in addition to the proton transfer (PT) process in the IP state, direct hydrogen abstraction process whose time constant was practically identical with the decay of ³BP* and the rise of the IP state was observed for BO3OD. That is, the apparent photoreduction profile of BO3OD was represented by the hybrid of Scheme 1a and the following direct reaction Scheme 2a of the competition between ET and HA.



The part of the BPH formation via the intra-IP PT in its whole yield was almost half, 0.51, in BO3OD. These

results indicated that dependences of ET and the direct HA or intra-IP PT reaction rates on the mutual distance and orientation of the reacting moieties and dynamics of changes in those mutual geometries regulated the apparent photoreduction mechanisms of the linked BP-DPA systems.

On the basis of the above findings, we have conducted more detailed investigations on the photoreduction processes of the linked BP-DPA systems with respect to the following problems: **1**, the solvent polarity effect which affects the dependences of the ET process on the mutual geometry,¹⁾ **2**, the solvent viscosity effect which will regulate the dynamic rearrangement of the mutual geometry, and **3**, temperature dependence of the photoreduction process which may be related to both **1** and **2**. In the following, by integrating obtained experimental results with those on the intermolecular hydrogen abstraction processes and mechanisms of the general ET phenomena, we will discuss the role of the ET reaction and/or the CT interaction in the hydrogen abstraction of BP* from the secondary amine.

Experimental

Apparatus and Samples. A picosecond laser photolysis system with a repetitive mode-locked Nd³⁺:YAG laser was used for transient absorption spectral measurements.^{25,26)} The third harmonic pulse (355 nm) with 22 ps fwhm was used for excitation. Synthesis and purification of 1-(4-anilinophenyl)-2-(4-benzophenoxy)ethane, (BP-O-(CH₂)₂-O-DPA), 1-(4-anilinophenyl)-3-(4-benzophenoxy)propane (BP-O-(CH₂)₃-O-DPA) and 1-(4-anilinophenyl)-8-(4-benzophenoxy)octane (BP-O-(CH₂)₈-O-DPA) were described elsewhere.²⁷⁾ Acetonitrile, benzene, and *N,N*-dimethylformamide (DMF) (Merck Uvasol) were used without further purification. All sample solutions were deaerated by repeated freeze-pump-thaw cycles. Since the change of the concentration of the sample from 5×10^{-3} to 2×10^{-2} M (1 M = 1 mol dm⁻³) did not affect the time evolution of the observed spectra, the intermolecular process seems negligible in the time regions investigated in the present work. In order to change the temperature, a hand-made apparatus combined with the temperature controller (Neslab, RTE-18) was used.

Extinction Coefficients of the Transient Species. The extinction coefficients used for the estimation of the reaction yields are as follows; 6500 M⁻¹ cm⁻¹ at 525 nm for ³BP*, 4600 M⁻¹ cm⁻¹ at 555 nm for BPH, and 31500 M⁻¹ cm⁻¹ at 690 nm for the IP state, ³(BP⁻...DPA⁺). Although detailed discussion on the determination of the extinction coefficient of each species was presented in the previous paper,¹⁵⁾ it is worth noting here the estimation of the BP⁻ extinction coefficient in the following.

Recently, Peters and Lee discussed²⁸⁾ the extinction coefficient of BP⁻ on the basis of the picosecond laser photolysis studies of the photoreduction process of BP with 1,4-diazabicyclo[2.2.2]octane (DABCO) in acetonitrile solution where no BPH formation takes place and only the charge separation (CS) reaction occurs. They compared the intensity of transient absorption spectrum of ³BP* in acetonitrile without DABCO and those of BP⁻ in the solution contain-

ing various concentration of DABCO (0.05–1.0 M) at 4 ns after the excitation with a picosecond 355 nm laser pulse. They found that the ratio of the intensity of the absorption of BP⁻ at an absorption maximum, ca. 715 nm, to that of ³BP* in the amine free solution decreased with increase of [DABCO]. They interpreted this decrease as due to the participation of ¹BP* in the quenching of the excited singlet state of BP by DABCO on the basis of our previous results on the photoreduction process of BP with various kinds of amines.^{17,19–21)} Since the singlet IP can undergo the effective charge recombination (CR) process, the relative yield of BP⁻ compared to ³BP* observed at long delay times may decrease as we have pointed out in previous papers.^{17,19–21)} Hence, qualitatively speaking, their interpretation is in accordance with our previous studies. By the comparison of the absorption intensity of ³BP* in amine free solution with those of BP⁻ in the solution containing DABCO whose concentrations are rather small, 0.05–0.1 M, they concluded that the extinction coefficient of BP⁻ is 0.92 times as large as that of ³BP*; in other word, the extinction coefficient of BP⁻ at an absorption maximum is smaller than that of ³BP*.

Although they compared simply the observed absorption intensities, their interpretation and analysis for the determination of the extinction coefficients are not clear, containing some problems. First, they used the time constant of 20 ps for the ¹BP* → ³BP* intersystem crossing (ISC) in acetonitrile solution on the basis of their picosecond laser photolysis studies. As was observed in the pioneering study by Hochstrasser et al.,²⁹⁾ it is well known that the transient absorption spectrum of ³BP* immediately after the excitation shows broad spectral shape, followed by the sharpening due to the cooling process in several tens of picosecond time region. These effects of the vibrationally hot state on the transient absorption spectrum and the time constant of the cooling have been reported for various kinds of molecules in solutions.^{26,30–32)} Hence, the determination of the ISC time constant should be carefully performed by taking into account the effect of the cooling process. In our previous studies on the determination of the ISC time constant by means of subpicosecond laser photolysis, the time profiles covering wide wavelength region were analyzed and the wavelength at which the effect of cooling process is small was selected. The ISC time constant thus obtained for ¹BP* in acetonitrile solution was 9 ps.¹⁷⁾ Recently, Tamai et al. reported the ISC time constant of 9.6 ps for ¹BP* in acetonitrile solution by applying the femtosecond transient grating method.³³⁾ The ISC time constant of 20 ps estimated by Peters and Lee, which is roughly twice longer than values estimated by us and by Tamai et al., seems to be mainly due to the cooling process. Accordingly, the estimation of the contribution from the singlet ion pairs in the absorption spectrum of BP⁻ based on this ISC time constant may not lead to the distinct conclusion. In addition, they ignored the contribution from the excitation of the CT complex between BP and DABCO formed in the ground state.

In order to avoid the ambiguity in the estimation, we have confirmed the correctness of our extinction coefficient in the following simple manner. The decay time profile of ³BP* absorbance obtained in the diluted solution of DABCO (<0.05 M) gives the decay time constant of ³BP* and, by extrapolation, the value of the absorbance at 0 ps if the time origin

is determined by the cross correlation or some other methods. In the condition where the decay time constant is not so short but more than nanosecond, such a severe determination of the time origin is not required for the estimation of the absorbance by extrapolation to 0 ps. Midpoint of the rise curve of the $S_n \leftarrow S_1$ absorbance of typical aromatic hydrocarbon can give the time origin with the experimental error less than the pulse width. By comparison of this extrapolated absorbance of ${}^3\text{BP}^*$ with the absorbance of BP^- at delay times when the quenching process has finished, we obtained the relative ratio of extinction coefficient of BP^- to that of ${}^3\text{BP}^*$ to be ca. 1.3. We have examined also effect of the DABCO concentration on this ratio and have confirmed that the ratio does not appreciably depend on the concentration of DABCO when it is not so high.¹⁸⁾ The same type of the comparison was performed for the photoreduction process of BP with *N,N*-diethyl-*p*-toluidine (DET) in acetonitrile, where only the production of the ionic species was observed as in the photoreduction of BP with DABCO in acetonitrile. Also in this system, the relative intensity of BP^- is ca. 1.45 times larger than that of the initial absorbance of ${}^3\text{BP}^*$ at absorption maxima.¹⁹⁾ Hence, the extinction coefficient of BP^- at an absorption maximum may be estimated to be 8500–9500 $\text{M}^{-1}\text{cm}^{-1}$ by assuming that the extinction coefficient of ${}^3\text{BP}^*$ is 6500 $\text{M}^{-1}\text{cm}^{-1}$ and all of the quenching results in the production of the ion pair. At any rate, the extinction coefficient of 10000 $\text{M}^{-1}\text{cm}^{-1}$ we have been employing for the absorption maximum of the BP^- has been confirmed by the above estimation.

Hence, we have used our previous values of the extinction coefficients for the analysis. Although the introduction of functional groups into BP and diphenylamine moieties may affect more or less the extinction coefficients of the transient species, the discussion and the interpretation on the experimental results and analysis may not be seriously affected by these substitutions.

Results and Discussion

Conformations of $\text{BP-O-(CH}_2)_n\text{-O-DPA}$ Systems. Prior to the discussion on the dynamic behaviors, we exhibit in Fig. 1 the distribution of the conformation of $\text{BP-O-(CH}_2)_n\text{-O-DPA}$ ($n=2, 3, 8$) at 20 °C calculated by means of the direct enumeration method weighted by the Boltzmann factor of each conformation.³⁴⁾ A part of these results are reported in the previous paper.²²⁾ The abscissa represents the distance between the oxygen of the carbonyl group of BP moiety and the hydrogen attached to the nitrogen atom of DPA moiety. The results for $n=3$ (middle frame) indicates that the distribution of the $\text{O}\cdots\text{H}$ distance may be divided roughly into two groups; the distribution at short distance with its maximum at ca. 6.5 Å and the more distant one with the maximum at ca. 13.5 Å. On the other hand, the result for $n=2$ (upper frame) does not show such a clear separation of the distribution into two groups, although several local maxima are observed. The averaged distance over the whole distribution for $n=2$ was 11.8 Å and that of $n=3$ for the distribution with the distance longer than 8 Å was 13.3 Å. Since this method of calculation does not include the effect of

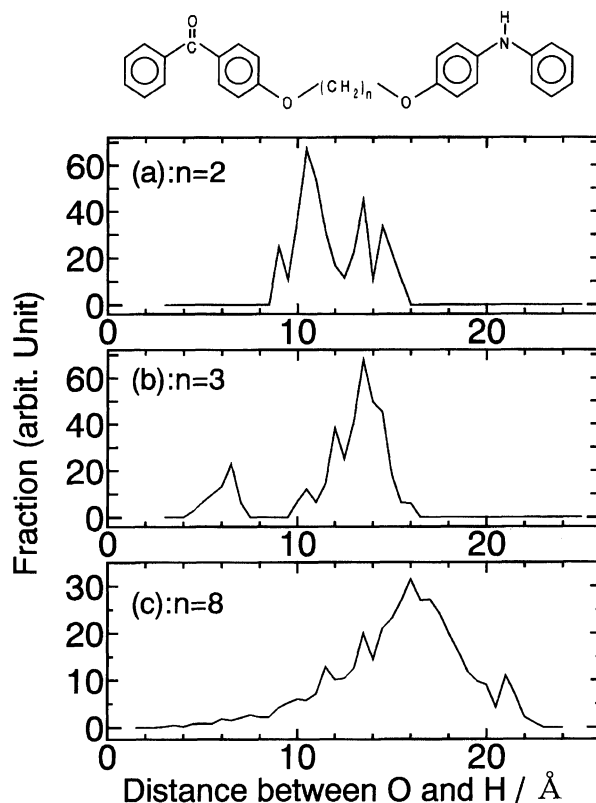


Fig. 1. Calculated distribution of the distance between the oxygen atom of carbonyl group of BP moiety and the hydrogen atom attached to the nitrogen of DPA moiety in $\text{BP-O-(CH}_2)_2\text{-O-DPA}$ (a), $\text{BP-O-(CH}_2)_3\text{-O-DPA}$ (b), and $\text{BP-O-(CH}_2)_8\text{-O-DPA}$ (c), (see text).

the solute-solvent interaction, it may not be adequate to quantitatively evaluate the fraction of each distance. However, it is worth noting here that the $n=3$ compound can take the distribution with shorter distance than $n=2$ compound.

In the case of $n=8$, wide and rather continuous distribution with the averaged distance at 16.0 Å was observed, indicating that, compared to the results of $n=2$ and $n=3$, the averaged distance is large and the geometrical restriction is rather loose. This result suggests that the mode of the reaction of BO8OD may be similar to those in the intermolecular reaction process, although its dynamics accompanied with thermal motion of the chain may be slowed down considerably.

Photoreduction Process of BO_nOD in Benzene Solution at Room Temperature. In benzene solution, the energy gap (ΔG) between ${}^3\text{BP}^*$ and the IP, BP^--DPA^+ , in the unlinked system is estimated to be +0.59 eV by means of the conventional procedures with the oxidation and reduction potentials of DPA and BP including the correction term for the solvation energy calculated by the Born equation.¹⁾ In this estimation, the inter-ionic distance was set to be 7 Å. Hence, the ET in such a loose configuration as observed in strongly polar solvents like acetonitrile^{1,37–41)} seems

rather difficult to take place in this non-polar solvent and geometrical rearrangements are required for the ET as well as the PT and hydrogen abstraction (HA) processes.

Figure 2 shows the time resolved transient absorption spectra of BO3OD in benzene solution at 22 °C, excited with a picosecond 355 nm laser pulse. Dotted line in the first frame shows the $T_n \leftarrow T_1$ absorption spectrum of 4-methoxybenzophenone (4MtBP) in benzene obtained in the amine-free condition. Time evolution of the absorption spectra indicates that $^3\text{BP}^*$ gradually decays together with the rise of new absorption bands at 555 and 740 nm. The former absorption at 555 nm can be assigned to the ketyl radical of BP moiety since the spectral band shape and its peak position are identical with those of ketyl radical of MtBP and related compounds.^{15,21,35} The latter absorption at 740 nm is ascribable to the neutral radical of hydrogen-abstracted DPA moiety since the absorption maximum and band shape are very close to those reported for unlinked DPA.^{15,21,35} Strong absorption around 700 nm due to the charge-separated state as observed in acetonitrile solution was not detectable in benzene solution.

Figure 3 shows the time profiles of $^3\text{BP}^*$ and BPH, obtained by the analysis of the observed spectra into these two species based on each reference spectrum. Solid lines in this figure are the calculated results based on the assumption that the HA reaction occurs without the participation of stable intermediate species such as the CS (IP or CT) state (direct reaction), indicating that the calculated curves reproduce the experimental results fairly well. Although the CS state was not clearly observed and the reaction process was repro-

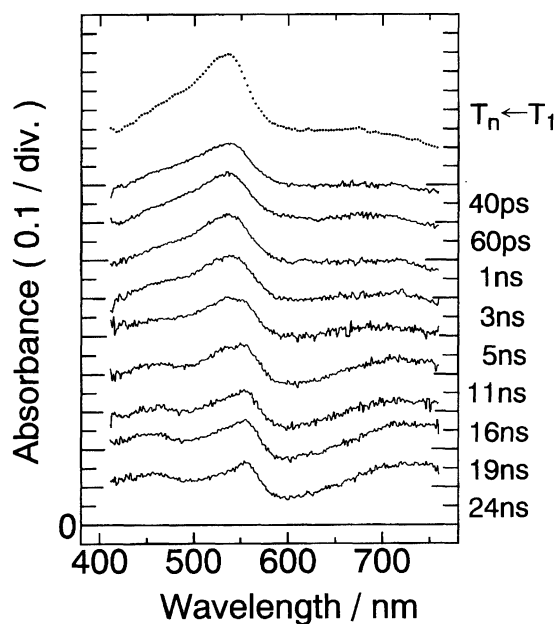


Fig. 2. Time-resolved transient absorption spectra of BP-O-(CH₂)₃-O-DPA in benzene solution excited with a picosecond 355 nm laser pulse.

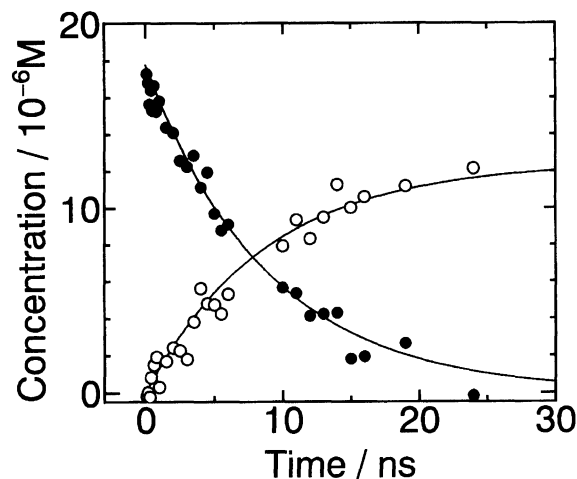


Fig. 3. Time profiles of $^3\text{BP}^*$ (●) and BPH (○) of BP-O-(CH₂)₃-O-DPA in benzene solution excited with a picosecond 355 nm laser pulse (see text). Solid lined are calculated curves based on Scheme 2a (see text).

duced by the direct reaction scheme as in the case of the reaction between unlinked $^3\text{BP}^*$ and DPA, there remains the possibility that the ultrashort lived intermediate CS state may participate in the reaction processes of both the unlinked¹⁵ and the linked systems of BP and DPA. Since the energy gap for CS between $^3\text{BP}^*$ and DPA at average distance in the present linked system was estimated to be positive as discussed above, it seems to take a long time for the intramolecular ET reaction, $^3\text{BP}^*-\text{DPA} \rightarrow (\text{BP}^--\text{DPA}^+)$. Presumably, a little change of the ground state conformation distribution will take place in the excited state, which facilitates the ET reaction. It seems to take a rather long time for this change of the conformation distribution, owing to the internal rotations around the spacer chains. However, immediately after the ET in a conformation with donor and acceptor in a close proximity to each other, ultrafast PT from cation to anion in the pair will be accomplished, which makes the detection of the intramolecular IP state extremely difficult. Anyhow, at the present stage of the investigation, it is rather difficult to definitely determine whether the HA proceeds via the two-step mechanism with real intermediate CS state or the direct HA mechanism with no observable intermediate CS state in benzene solution. The extremely short lifetime of the intermediate CS state in the former mechanism can be deduced also from the fact that, even though the summation of the extinction coefficients of the absorption bands of BP⁻ and DPA⁺ locating around 700 nm is several times larger than those of $^3\text{BP}^*$ and BPH radical, the CS state was not observed. Similar results were obtained also for BO2OD and BO8OD in benzene solution.

The lifetimes of $^3\text{BP}^*$ and the reaction yields for BO n OD ($n=2, 3$, and 8) are listed in Table 1, indicating that the decay time constant of $^3\text{BP}^*$ for BO3OD

Table 1. The Time Constants and Reaction Yields of Photoreduction Processes of BO2OD, BO3OD, and BO8OD in Benzene Solution, Obtained by the Direct Reaction Scheme 2a (See Text)

	BO2OD	BO3OD	BO8OD
Lifetime of $^3\text{BP}^*$	15.2 ns	9.0 ns	10.5 ns
Yield of "direct" BPH production	0.69	0.74	0.54

Experimental errors for each value, except for the systematic ones arising from the estimation of the extinction coefficients of the transient species, were estimated to be ca. $\pm 10\%$.

is the shortest among these three systems and that for BO2OD is the longest. This result of the dependence of the lifetimes on the length of the methylene chain is closely related to the systematic investigations on the photoinduced charge separation (CS) process of electron donor (D) and acceptor (A) systems linked by methylene chains,^{1,37-41)} such as 4-(dimethylamino)phenyl-(CH₂)_n-(1-pyrenyl) ($n=1, 2, 3$: P_n) and 4-(dimethylamino)phenyl-(CH₂)_n-(9-anthryl) ($n=1, 2, 3$: A_n). These studies on the CS process of linked D-A systems have revealed that, in non-polar solutions such as hexane, the effective CS was observed only for $n=3$ systems and the CS time constants were in the order of several nanoseconds. These results on linked D-A systems indicate that compact sandwich-like conformation is required for the CS in nonpolar solutions to take place and the CS rate constants are regulated mainly by the geometrical rearrangement process. Present experimental results may be consistent with those results of the intramolecular exciplex formation of P_n and A_n in nonpolar solvents, since the dynamical rearrangement to take a compact conformation favorable for the reaction in the excited state is necessary in non-polar solvent, in either case of the participation of the ultrashort intermediate CS state in the two-step reaction process or the direct HA.

The yield of BPH radical in BO8OD is slightly smaller than those in BO2OD and BO3OD as shown in Table 1. Presumably, the deactivation into the ground state competing with the ET or HA will take place depending on the geometry at the close approach of the $^3\text{BP}^*$ and DPA groups to each other and this geometry might be affected by the chain length. At the present stage of the investigation, however, the reason for this result is not evident.

Photoreduction Processes of BO_nOD in Acetonitrile Solution at Room Temperature. As stated in the introductory section and in our previous studies in acetonitrile solution at 22 °C,²²⁾ it was demonstrated that almost all (>90%) production of BPH radical took place via the consecutive two-step reaction mechanism (Scheme 1a) for BO2OD. On the other hand, the photoreduction profile of BO3OD was interpreted by the hybrid mechanism of Scheme 1a and

the direct reaction Scheme 2a. To elucidate the influence of geometrical restriction on the apparent reaction mechanism in a more detail, we have studied the photoreduction process of BO8OD in the present work.

In Fig. 4, we show time-resolved transient absorption spectra of BO8OD in acetonitrile solution at 22 °C, excited with a picosecond 355 nm laser pulse. Dotted line in the first frame is the T_n ← T₁ absorption spectrum of 4-methoxybenzophenone (4MtBP) measured in the amine free condition. Time evolution of the absorption spectra in Fig. 4 indicates that the absorbance due to $^3\text{BP}^*$ moiety gradually decays, together with the rise of new absorption band at 555 and 700 nm. The absorption at 555 nm can be assigned to the ketyl radical of BP moiety. The latter 700 nm absorption spectrum can be ascribed to the overlapped one of DPA⁺ and BP⁻ absorption bands on the basis of the spectra reported previously.^{15,22,42)} The absorption signal due to the IP state at 700 nm increases in the initial time region of several nanoseconds, followed by the decrease. No remarkable evolution of the absorption spectra was observed in the time region longer than ca. 20 ns after the excitation.

In order to elucidate the time profile of each species, $^3\text{BP}^*$, BPH, and IP state, the observed absorption spectra were analyzed into these three species on the basis of each reference spectrum, results of which are shown in Fig. 5. The ordinate of this figure represents the concentration obtained by using the extinction coefficient of each species given in the experimental section. Solid lines in Fig. 5a represent the time profiles calculated on the basis of the consecutive reaction Scheme 1a. In this calculation, the decay of $^3\text{BP}^*$ was assumed to be expo-

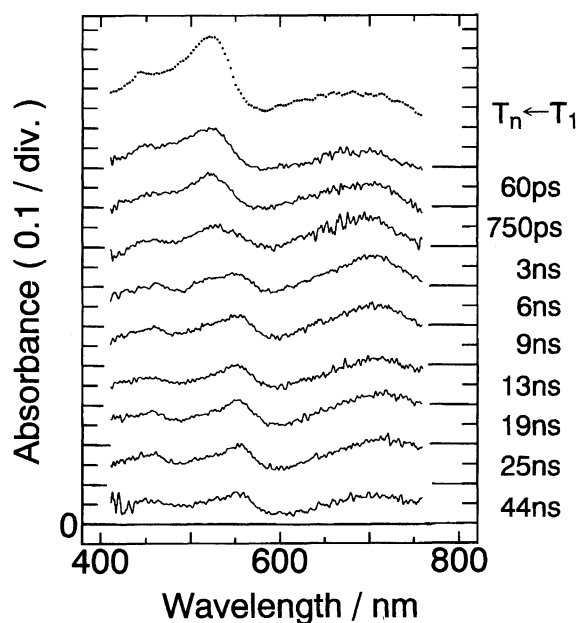


Fig. 4. Time-resolved transient absorption spectra of BP-O-(CH₂)₈-O-DPA in acetonitrile solution excited with a picosecond 355 nm laser pulse.

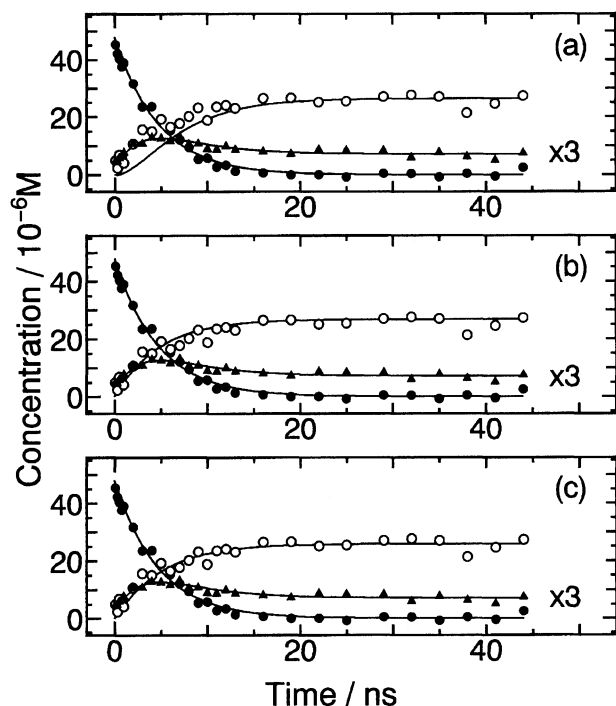


Fig. 5. Time profiles of $^3\text{BP}^*$ (●), BPH (○), and IP state (▲) of BP-O-(CH₂)₈-O-DPA in acetonitrile solution excited with a picosecond 355 nm laser pulse. Solid lines are calculated curves based on consecutive reaction Scheme 1a for (a), direct reaction Scheme 2a for (b), and hybrid model of Schemes 1a and 2a for (c), where the contribution of the Scheme 1a is 15%, (see text).

nential. In addition, parameters of the transient species such as lifetimes and reaction yields were determined in such a manner that the time profiles of $^3\text{BP}^*$ and IP were consistent with each other in Scheme 1a since the time profile of IP state can be most clearly identified as shown in Fig. 4.

As Fig. 5a shows, the calculated curves based on the consecutive reaction Scheme 1a does not satisfactorily reproduce the experimental results with respect to the rise profile of BPH. The deviation of the calculated time profile of BPH from the experimental results in such a way that the experimental results are always larger than the calculated curve in the course of the formation of BPH indicated that some part of BPH was formed rapidly prior to the decay of the IP state. In addition, it was necessary to assume the value of 2.2 for the reaction yield of the intra-IP PT process in order to reproduce the final yield of BPH. Although this absurd value may be partly due to errors in the estimation of the extinction coefficients of the transient species, this unreasonableness is beyond such errors. In view of the deviation of the calculated time profile of the rise of BPH from the observed one and the absurd value of the reaction yield, it may be concluded that the reaction Scheme 1a is not adequate for the reaction of BO8OD in acetonitrile, although this Scheme 1a was suitable

for BO2OD and intermolecular reaction of $^3\text{BP}^*$ and tertiary amines in acetonitrile solution.

On the other hand, the calculated results based on the reaction Scheme 2a show better agreement with the experimental results for the time profiles of three species as exhibited in Fig. 5b. This result indicates that most of the BPH formation occurs with the time constant identical with the decay of $^3\text{BP}^*$ and the decay time constant of the IP state is not very much correlated with the rise profile of BPH. Although it was found that most of the BPH formation took place via the Scheme 2a, we have applied also the hybrid mechanism for the analysis of the experimental results of BO8OD in acetonitrile, results of which are shown in Fig. 5c. From these simulations, the contribution of the intra-IP PT process to the whole BPH production was estimated to be less than 15%. At any rate, it may be concluded that most of the BPH production (>85%) occurs with the time constant identical with the decay of $^3\text{BP}^*$ for BO8OD in acetonitrile solution at room temperature.

It should be noted here that, in polar solution, not all of the IP have disappeared in the time domain presented here. Actually, it was observed by the nanosecond laser photolysis studies²⁷⁾ that the long-lived IP decayed in microsecond time domain. The investigation of the magnetic field effect on the decay process predicted that the conformation with a large distance between BP⁻ and DPA⁺ moieties may be responsible for such a long-lived IP state. It seems possible that the long-lived IP is produced either by the initial quenching process of $^3\text{BP}^*$ via a rather long distance ET or during the conformational rearrangement process of the IP in competition with the intra-IP proton transfer. At the present stage of the investigation, however, it is difficult to discriminate clearly these formation pathways of the long-lived IP. In anyway, the contribution from the long-lived IP to the total yield of the IP is small and we have analyzed here the experimental results by assuming the long-lived IP formation during the conformational rearrangement process in competition with the intra-IP proton transfer.

Lifetimes and the reaction yields related to the photoreduction of BO8OD are listed in Table 2, where the results of BO2OD and BO3OD are also collected. As shown in this table, rates of the decay of $^3\text{BP}^*$ moiety and the proton transfer in the IP state and even the reaction mechanisms are dependent on the length of the chain. In addition, these results in acetonitrile solution are quite different from those in benzene solution as shown in Table 1.

Photoreduction Processes of BO n OD in DMF Solution at Room Temperature.

Although the dielectric constants of DMF and acetonitrile are almost the same, 36.7 for DMF and 37.5 for acetonitrile at 20 °C, viscosity of DMF is almost three times as large as that of acetonitrile. Hence, the photoreduction processes of BO n OD in DMF solution may provide the in-

Table 2. The Time Constants and Reaction Yields of Photoreduction Processes of BO2OD, BO3OD, and BO8OD in Acetonitrile Solution, Obtained by the Hybrid Model of Schemes 1a and 2a (See Text)

	BO2OD	BO3OD	BO8OD ^{b)}
(Reaction profile of ³ BP*)			
Lifetime of ³ BP*	0.95 ns	1.75 ns	4.75 ns
Yield of "direct" BPH production	0.07	0.30	0.49
Yield of the stable IP formation	0.65	0.35	0.25
(Reaction of the stable IP) ^{a)}			
Lifetime of the stable IP	9.55 ns	2.75 ns	3.0 ns
Yield of the intra-IP PT	1.00	0.90	(0.4)
Yield of the long-lived IP	0.16	0.18	0.19
Contribution of the PT in the stable IP to the whole HA reaction	0.90	0.51	(<0.15)

Experimental errors for each value, except for the systematic ones arising from the estimation of the extinction coefficients of the transient species, were estimated to be ca. $\pm 10\%$. a) The summation of the each reaction yield over unity may be due to over- or underestimation of the extinction coefficients of the transient species. b) In the case of BO8OD, the production yield of IP from ³BP* was low, so that the evaluation of the contribution from the intra-IP PT to the whole yield of the ketyl radical production was rather difficult.

formation concerning the effect of the solvent viscosity on the photoreduction process.

Exhibited in Fig. 6 are time-resolved transient absorption spectra of BO3OD in DMF solution at 22 °C, excited with a picosecond 355 nm laser pulse. Dotted line in the first frame is the $T_n \leftarrow T_1$ absorption spectrum of 4-methoxybenzophenone (4MtBP) measured in the amine free condition. Time evolution of the absorp-

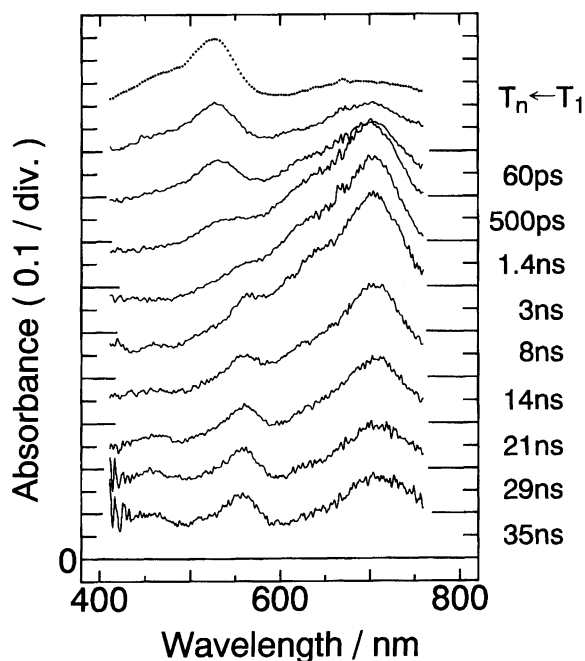


Fig. 6. Time-resolved transient absorption spectra of BP-O-(CH₂)₃-O-DPA in DMF solution excited with a picosecond 355 nm laser pulse.

tion spectra in Fig. 6 indicates that the absorption due to ³BP* moiety gradually decreases along with the rise of new absorption band at 700 nm ascribable to the overlapped one of DPA⁺ and BP⁻ and that at 555 nm due to the BPH radical. The absorption signal due to the IP state at 700 nm increases in the time region of a few ns, followed by the decrease in the time region of a few tens of ns. The absorption signal due to BPH at 555 nm can be also observed in the time region of tens of ns. No remarkable evolution of the absorption spectra can be observed in the time region longer than ca. 30 ns after the excitation.

In order to elucidate the time profile of each species, ³BP*, BPH, and IP state, the observed absorption spectra were analyzed into the spectra of these species in the same manner as performed in Fig. 5, results of which are shown in Fig. 7. Solid lines in Fig. 7 represent the results calculated on the basis of the hybrid mechanism, indicating that the experimental results are well reproduced by the calculated results. The application of the consecutive reaction Scheme 1a or direct reaction Scheme 2a did not satisfactorily reproduce the experimental results.

Lifetimes and the reaction yields in the photoreduction of BO3OD are listed in Table 3, where the results of BO2OD and BO8OD are also collected. Although the reaction profiles depending on the chain length are more similar to those in acetonitrile solution rather than those in benzene, there are still some differences between these two polar solutions with respect to the IP production and the direct BPH formation in the quenching process of ³BP* and the lifetime of the IP state. In the following, we will discuss the solvent po-

Table 3. The Time Constants and Reaction Yields of Photoreduction Processes of BO2OD, BO3OD, and BO8OD in DMF Solution, Obtained by the Hybrid Model of Schemes 1a and 2a (See Text)

	BO2OD	BO3OD	BO8OD
(Reaction profile of $^3\text{BP}^*$)			
Lifetime of $^3\text{BP}^*$	0.35 ns	1.55 ns	9.50 ns
Yield of "direct" BPH production	0.00	0.12	0.35
Yield of the stable IP formation	0.55	0.46	0.32
(Reaction of the stable IP) ^{a)}			
Lifetime of the stable IP	> 50 ns	13.5 ns	11.8 ns
Yield of the intra-IP PT	1.20	1.15	1.0
Yield of the long-lived IP	0.15	0.14	0.18
Contribution of the PT in the stable IP to the whole HA reaction	1.00	0.84	0.48

Experimental errors for each value, except for the systematic ones arising from the estimation of the extinction coefficients of the transient species, were estimated to be ca. $\pm 10\%$. a) The summation of the each reaction yield over unity may be due to over- or underestimation of the extinction coefficients of the transient species.

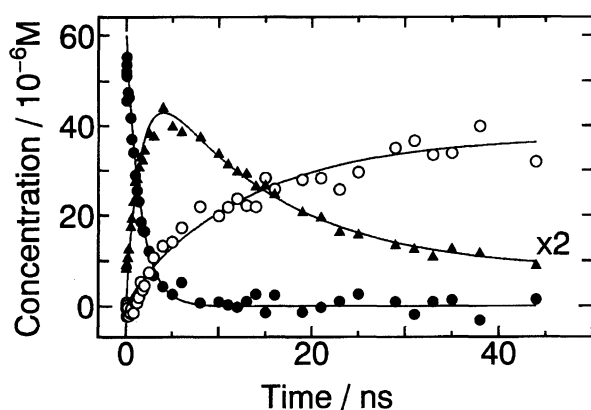


Fig. 7. Time profiles of $^3\text{BP}^*$ (●), BPH (○), and IP state (▲) of BP-O-(CH₂)₃-O-DPA in DMF solution excited with a picosecond 355 nm laser pulse. Solid lines are calculated curves based on hybrid model of Schemes 1a and 2a, where the contribution of the Scheme 1a is 85%, (see text).

larity and viscosity effects on the photoreduction process, considering also the effect of the chain length on the reaction.

Solvent and Chain Length Dependence of the Photoreduction Process. As indicated in Tables 1, 2, and 3, chain length, solvent polarity, and viscosity affect the rate constant of each process and even the reaction mechanism. The proton transfer (PT) process following the charge separation (CS) took place in strongly polar solvents and the degree of the contribution from the intra-IP PT process in the whole hydrogen abstraction process varies depending on the chain length and the solvent, while such PT process in the CS state was not observed in benzene solution nor in the intermolecular hydrogen abstraction reaction be-

tween $^3\text{BP}^*$ and DPA in polar as well as in nonpolar solutions. In order to interpret these results depending on many factors, we will discuss the differences among these systems in the dynamic behaviors after the excitation in the following.

First, we concentrate our discussion on the solvent effects on the quenching process of $^3\text{BP}^*$ of BO n OD. The lifetime of $^3\text{BP}^*$ of BO2OD was longest among these three systems of BO n OD ($n=2, 3$ and 8) in benzene solution. As stated in the previous subsection, this chain length dependence of the $^3\text{BP}^*$ lifetime indicates that the geometrical rearrangement to take a compact form favorable for the reaction between $^3\text{BP}^*$ and DPA is necessary for the quenching process in benzene solution.

On the other hand, the effect of the chain length on the lifetime of $^3\text{BP}^*$ was quite different in strongly polar solutions as shown in Tables 2 and 3. The $^3\text{BP}^*$ lifetime of BO2OD is shortest and the quenching process is mainly due to the CS to produce the stable IP state (IP) in BO2OD. Moreover, the lifetime of $^3\text{BP}^*$ of BO2OD in DMF solution is about three times shorter than that in acetonitrile although the viscosity of DMF is much higher. This result indicates that the geometrical rearrangement does not play an important role in the quenching process of $^3\text{BP}^*$ moiety of BO2OD in strongly polar solutions and is in qualitatively consistent with the previous results on the photoinduced CS processes of electron donor (D)-acceptor (A) linked by methylene chains^{1,37-41)} in strongly polar solutions. In these investigations, it was demonstrated that the CS in P_{*n*} and A_{*n*} occurred in the time domain of a few — a few tens of a picosecond and the CS rate constant decreased with increase of the methylene chain.^{1,39-41)} These results show that, in polar solutions, CS can oc-

cur in a loose configuration without large geometrical rearrangement to attain a compact structure^{1,37-41)} and the decrease of the rate constant with increase of the methylene chain is caused by the decrease of the electronic tunneling matrix element.^{1,39,40)}

The difference of the ET rate of BO2OD between these two polar solutions may be related to the difference in the solvent reorganization energy, λ_s , in the ET process. Although the static dielectric constants of DMF and acetonitrile are almost the same, the refractive index of DMF is ca. 10% larger. Therefore, on the basis of the equation by Marcus,^{2,42)} the λ_s in DMF solution for the CS is smaller than that in acetonitrile solution. Since ΔG for the CS between $^3\text{BP}^*$ and DPA in these two solvents, which is estimated to be ca. -0.29 eV, is in the normal uphill region, the decrease in λ_s increases the CS rate constant. From this reasoning, it is concluded that the lifetime of $^3\text{BP}^*$ moiety of BO2OD in DMF solution is shorter than that in acetonitrile solution.

On the basis of the above results and discussion and by taking into account the fact that the conformation rearrangement process is in competition with the CS process in loose configurations in strongly polar solutions, we can classify the competition between the reaction and the dynamic geometrical rearrangements into two cases. First, in case where the time constant of the CS in loose configuration is much faster than the average time staying at a certain geometry (fast CS case), the probability for $^3\text{BP}^*$ moiety to undergo the CS process with DPA moiety may be large while the direct BPH production may have only small possibility. The quenching of $^3\text{BP}^*$ of BO2OD in strongly polar solutions may be regarded as one of the examples of this extreme case. On the other hand, when the CS reaction rate constant in loose configuration is small and/or the dynamic rearrangement process to find suitable configurations for rapid BPH production is fast compared to the above CS process (slow CS case), the latter process predominates. The reaction mechanism in benzene solutions may be the example of this case.

According to the above classification, the reaction of BO3OD in strongly polar solutions may be regarded as an intermediate case and the difference of the reaction mechanism between DMF and acetonitrile solutions may be interpreted as follows. Although the quenching of the $^3\text{BP}^*$ moiety of BO3OD are mainly due to the CS and the BPH production in both of these two polar solvents, the CS has larger contribution in DMF solution than in acetonitrile. This result may be interpreted as due to the high viscosity to slow down the dynamic geometrical rearrangement processes and the small λ_s to accelerate the CS process in DMF. As a result, although the contribution of the direct BPH production to the quenching of $^3\text{BP}^*$ in DMF solution decreased, the total the quenching rate was comparable with that in acetonitrile solution owing to the increase

in the CS rate constant.

The above interpretation seems applicable also to the dynamic behaviors of BO8OD by considering that the average distance between the BP and DPA moieties is rather large and the geometrical restriction is rather loose. By comparing the lifetime of $^3\text{BP}^*$ of BO8OD in acetonitrile with that in DMF, one can find that the lifetime in DMF solution is twice as long as that in acetonitrile, while those of BO3OD are almost the same and, in the case of BO2OD, the lifetime is considerably shorter in DMF, i.e., the quenching in DMF is much more effective. This result indicates that the importance of the geometrical rearrangement to take configurations with closer approach of $^3\text{BP}^*$ and DPA groups in the quenching process of $^3\text{BP}^*$ increases with increase of the chain length even in strongly polar solvents. That is especially the case for BO8OD, since the averaged mutual distance is rather long in BO8OD. Although the lifetime of $^3\text{BP}^*$ in DMF solution is longer than that in acetonitrile, the percentage of the CS process in the whole quenching process of $^3\text{BP}^*$ is larger than in acetonitrile solution as it is the case for BO3OD. This result seems to support the interpretation based on the competition of the dynamic rearrangements with the CS in loose configurations, since the CS is more feasible but dynamic change in the configuration is slower in DMF.

In addition, one more point to be addressed regarding the photochemical reactions of BO8OD is that the yield of the direct BPH production is the largest among the three systems of $\text{BO}n\text{OD}$ ($n=2, 3, 8$) in both acetonitrile and DMF solutions. This result seems to be related also to the degree of the restriction in geometries and their dynamic rearrangements in the excited state. Since the geometrical restriction in BO8OD is rather loose and distributed in wide range, the possibility to find some suitable geometry with short O...H distance may increase. Moreover, the increase in the methylene chain length may affect also the mode of motions in the conformational rearrangements to take a compact geometry favorable for the reaction in the excited state, since the distribution is rather continuous. At any rate, the competition of the CS process with the geometrical rearrangement seems to affect the dynamic behaviors also in BO8OD.

Although the time constant of the PT process in the IP state depends also on the length of the chain and the solvent, its dependence on the length of the chain in each of the strongly polar solutions is similar to that of the decay time constant of $^3\text{BP}^*$ moiety in benzene solution; the time constant of BO3OD was comparable with that of BO8OD, while the time constant in BO2OD was much longer than those of BO3OD and BO8OD. Since the PT process is much more sensitive to the geometry in the IP state, geometrical rearrangements in the IP state seems to play an important role in the intra-IP PT reaction as in the case of the quenching

process of $^3\text{BP}^*$ moiety in benzene solution. Actually, the PT time constant of each BOnOD in viscous DMF solution is longer than that in acetonitrile. Accordingly, although the distributions of the geometry of the IP produced by the ET seem to be dependent on the solvents and the length of the chain, the chain-length dependence of the PT rate in the IP state in polar solutions is similar to that of the quenching of $^3\text{BP}^*$ moiety in nonpolar solution in a qualitative sense, probably because both processes require the geometrical rearrangements to compact conformations.

Temperature Dependences of the Reaction Processes in Acetonitrile Solution In order to confirm the above interpretation, we have investigated the temperature effect on the dynamic behaviors of BO3OD in acetonitrile solutions result of which are indicated in Table 4. The temperature dependence of the extinction coefficient of each species was not taken into account in the analysis. The change of the extinction coefficient due to such small range of temperature variation without phase transition from liquid to solid may be rather minor.

The probability of the CS in the quenching process of $^3\text{BP}^*$ increases with decrease of the temperature as shown in Table 4. This result seems to support the interpretation given in the previous subsection, since the temperature lowering increases the solvent viscosity and the solvent polarity resulting in the decrease of the relative possibility of the direct hydrogen atom transfer and the increase of the CS process in loose configuration. In addition, the PT rate in the IP state decreases by temperature lowering, which is due to the increase of the viscosity. On the other hand, the opposite tendency was observed with increase of the temperature. Summarizing above results, it may be concluded that the interpretation given for the solvent dependence of the dynamic behavior is consistent with the results of the investigations on its temperature dependence.

Difference between the Reaction Mechanisms of Linked and Unlinked Systems. As stated in the introductory section and in previous papers,^{15,16)} the PT process in the IP state was not observed in the intermolecular photoreduction process of BP with DPA and other secondary as well as primary amines in nonpolar and polar solutions at room temperature. The time constant of the production of BPH radical is identical with the decay of $^3\text{BP}^*$ and the rise of the IP state as shown in the Scheme 1. In addition, the yield of the direct BPH production during the quenching process of $^3\text{BP}^*$ is more than 70% for the reaction of $^3\text{BP}^*$ with primary and secondary amines in solutions at room temperature; the dominant quenching mechanism of $^3\text{BP}^*$ is due to the direct BPH production. The IP state produced in competition with the BPH formation undergoes the ionic dissociation without the BPH formation in strongly polar solutions.

The fact that the PT process in the IP state or the

charge-separated (CS) state was not observed in the intermolecular reaction between $^3\text{BP}^*$ and secondary and primary amines in solutions at room temperature is partly due to the small yield of the production of the IP or CS state during the quenching process of $^3\text{BP}^*$, which makes it rather difficult to observe the time profiles of the IP or the CS state clearly; in nonpolar solutions, the yield is much smaller than 10%. In addition, the ionic dissociation process determines the lifetime of the triplet IP state in strongly polar solution; in acetonitrile solution at room temperature, the rate constant of the ionic dissociation is ca. $0.5\text{--}2 \times 10^9 \text{ s}^{-1}$.⁴⁴⁾ However, it should be noted that the yield of the direct BPH production during the quenching process of $^3\text{BP}^*$ is more than 70% for the intermolecular reaction of $^3\text{BP}^*$ with primary and secondary amines in solutions at room temperature. Even if the PT process in the IP contributes to the whole hydrogen abstraction process in the intermolecular reaction, the dominant pathway for the BPH production in the intermolecular reaction is due to the direct abstraction.

The above difference between the HA mechanisms of the linked and un-linked systems may be interpreted also by the dependences of the ET and direct HA or PT reaction rates on the mutual distance and orientation of the reacting moieties, and the dynamics of changes in those mutual geometries in the excited state. In the case of the unlinked systems in solutions of usual viscosity, rotational and translational motions of two reacting molecules are usually much faster than those in the linked systems. When the ET process at a certain geometry is slower than the average time for geometry change to take some structures with shorter distance and favorable orientation between reactants, the possibility that the reaction may start at a configuration more favorable for the reaction is higher in the unlinked systems. In addition, if the geometry for ET is also preferable for the subsequent PT process after taking such favorable conformations, the possibility of the rapid BPH production increases. In the extreme case where the PT following the ET may proceed prior to the solvation of the produced IP or in the partial charge transfer state before full charge transfer is attained by a slight geometrical change, it may be difficult to assign whether the reaction mechanism is direct or consecutive as discussed already to some extent in the previous section. The encounter complex with unfavorable structure for the PT may terminate in the production of the stable IP state which undergoes ionic dissociation competing with PT depending on the polarity of the solvent. In fact, the intermolecular ET distance depending on the energy gap of the CS reaction, $-\Delta G_{\text{CS}}$, producing the IP affects the subsequent PT process in the intermolecular HA reaction of $^3\text{BP}^*$ from *tertiary* aromatic amines in acetonitrile.^{17–21)}

On the basis of the above interpretation, we are now going on investigating the intermolecular HA process

Table 4. Temperature Dependence of the Time Constants and Reaction Yields of Photoreduction Processes of BO3OD in Acetonitrile Solution, Obtained by the Hybrid Model of Schemes 1a and 2a (See Text)

	-20 °C	22 °C	50 °C
(Reaction profile of ³ BP*)			
Lifetime of ³ BP*	2.75 ns	1.75 ns	0.92 ns
Yield of "direct" BPH production	0.22	0.30	0.35
Yield of the stable IP formation	0.38	0.35	0.30
(Reaction of the stable IP) ^{a)}			
Lifetime of the stable IP	15.5 ns	2.75 ns	1.65 ns
Yield of the intra-IP PT	0.90	0.90	0.62
Yield of the long-lived IP	0.08	0.18	0.24
Contribution of the PT in the stable IP to the whole HA reaction	0.67	0.51	0.35

Experimental errors for each value, except for the systematic ones arising from the estimation of the extinction coefficients of the transient species, were estimated to be ca. $\pm 10\%$. a) The summation of the each reaction yield over unity may be due to over- or underestimation of the extinction coefficients of the transient species.

from *secondary* amines in strongly polar solvent at low temperature where the rotational and translational motions are slow but the ET rate will be comparable to that at room temperature due to the increase of the solvent polarity, change of reaction exothermicity, etc. Preliminary result⁴⁵⁾ that the decrease of the yield of the "direct" HA and the increase of the yield of the IP were observed with the temperature lowering may indicate that the intermolecular ET takes place prior to taking closer geometry between the reactants where the PT after ET is feasible.

Concluding Remarks

The results of the present picosecond laser photolysis studies on the intramolecular photoreduction processes of BP by DPA linked by spacers demonstrate clearly that the apparent mechanisms of HA reaction are strongly dependent on the length of the chain, polarity and viscosity of solvents, and temperature. These complex behaviors may be interpreted consistently from the viewpoints that the CS reaction in loose configuration which is more feasible for larger energy gap, $-\Delta G_{CS}$, and in polar solvent takes place in competition with the dynamic rearrangement processes to a more compact conformation favorable for the reaction and that the mutual distance and orientations between the ³BP* and DPA groups immediately before the reaction are of crucial importance in determining the apparent reaction mechanisms, i.e., the direct HA, the IP formation by CS followed by PT, and the IP formation followed by ionic dissociation without PT in polar solutions. Moreover, even in the case of the "direct HA", it seems quite feasible that, immediately after the CS in a conformation with donor and acceptor in a close prox-

imity to each other in a favorable orientation for PT, ultrafast PT in the pair will take place, which makes the detection of the IP state extremely difficult.

The above general consideration on the photoinduced ET mechanisms of the HA reaction between BP and DPA are closely related to our previous investigations on the singlet exciplex systems leading to the concepts of "loose" and "compact" exciplexes and/or IP's depending upon solvent polarities and $-\Delta G_{CS}$, etc.^{1,37-41,46)} It should be noted here that very detailed studies concerning the solvent polarity effects on the geometrical and electronic structures of the exciplex state have been conducted recently by employing the A-D systems linked by rigid, semi-rigid and flexible saturated hydrocarbon spacers,^{47,48)} results of which clearly support those concepts proposed previously.^{1,37-41,46)} Moreover, recent investigations on the solvent dependence of intramolecular proton transfer, fluorescence, intersystem crossing, and nonradiative decay in styrene-amine exciplexes show clearly that the observed results can be attributed to a change in exciplex conformation from compact (folded) one in nonpolar solvents to loose (extended) one in polar solvents.⁴⁹⁾

On the other hand, picosecond laser spectroscopic⁵⁰⁾ and theoretical²³⁻²⁵⁾ studies on the intermolecular photoinduced ET reaction in polar solutions have extended our views to include donor-acceptor distance distributions in the photoinduced CS process leading to the formation of various geminate ion pairs and exciplexes with different geometries and established the mechanism of the $-\Delta G_{CS}$ dependence of the inter-ionic distance distribution in the geminate IP's, which is essential for the interpretation of the apparent lack of the inverted region in the fluorescence quenching reaction

due to CS in polar solutions. In this respect, it should be emphasized here that our previous results on the reduction of $^3\text{BP}^*$ by tertiary aromatic amines in acetonitrile solution demonstrated that the rate constant of the intra-IP PT reaction significantly decreased with increase of $-\Delta G_{\text{CS}}$ for the ^3IP formation, indicating the increase of the interionic distance in ^3LIP with increase of $-\Delta G_{\text{CS}}$ ^{17,19–21}) in accordance with theoretical studies.^{23–25}) When *N,N*-diethyl-*p*-toluidine was used as hydrogen donor, $-\Delta G_{\text{CS}}$ was very large, which resulted in practically no intra-IP PT reaction but only the ionic dissociation in acetonitrile solution.^{19,20}) These results are also important examples of the fact that the mutual geometry between $^3\text{BP}^*$ and amine immediately before the reaction is of essential importance in determining the apparent reaction mechanisms.

This work was partly supported by Grant-in-Aids from the Ministry of Education, Science and Culture to N. M (No. 62065006) and to H. M (No. 03640409. 05640570).

References

- 1) a) N. Mataga and M. Ottolenghi, "Molecular Association," ed by R. Foster, Academic Press, New York (1984), Vol. 2, p. 1; b) N. Mataga, *Pure Appl. Chem.*, **56**, 1255 (1984); c) N. Mataga, *Pure Appl. Chem.*, **65**, 1606 (1993); d) N. Mataga and H. Miyasaka, *Prog. React. Kinet.*, **19**, 317 (1994).
- 2) R. A. Marcus and N. Sutin, *Biochem. Biophys. Acta*, **811**, 265 (1985).
- 3) I. Rips, J. Klafter, and J. Jortner, "Photochemical Energy Conversion," ed by J. R. Norris and D. Meisel, Elsevier, New York (1988), p. 1.
- 4) M. Maroncelli, J. McInnis, and G. R. Fleming, *Science*, **243**, 1674 (1989).
- 5) P. F. Barbara and W. Jarzeba, *Adv. Photochem.*, **15**, 1 (1990).
- 6) Some other reviews of recent development: a) "Perspectives in Photosynthesis," ed by J. Jortner and B. Pullman, Kluwer Academic, Dordrecht (1990); b) "Electron Transfer in Inorganic, Organic and Biological Systems," ed by J. R. Bolton, N. Mataga, and G. McLenden, in "Advances in Chemistry Series 228," American Chemical Society, Washington, DC (1991); c) "Dynamics and Mechanism of Photoinduced Electron Transfer and Its Related Phenomena," ed by N. Mataga, T. Okada, and H. Masuhara, Elsevier, Amsterdam (1992).
- 7) A. Beckett and G. Porter, *Trans. Faraday Soc.*, **59**, 2038 (1963).
- 8) G. Porter and M. R. Topp, *Proc. R. Soc. London, Ser. A*, **315**, 163 (1970).
- 9) S. G. Cohen, A. Parola, and G. H. Rarsons, *Chem. Rev.*, **73**, 1411 (1973).
- 10) S. Arimitsu and H. Masuhara, *Chem. Phys. Lett.*, **22**, 543 (1973).
- 11) S. Arimitsu, H. Masuhara, N. Mataga, and H. Tsubomura, *J. Phys. Chem.*, **79**, 1255 (1975).
- 12) K. S. Peters, S. C. Felich, and C. G. Shaefer, *J. Am. Chem. Soc.*, **102**, 5701 (1980).
- 13) L. E. Manring and K. S. Peters, *J. Am. Chem. Soc.*, **107**, 6452 (1985).
- 14) M. Hoshino and M. Kogure, *J. Phys. Chem.*, **93**, 728 (1989).
- 15) H. Miyasaka and N. Mataga, *Bull. Chem. Soc. Jpn.*, **63**, 131 (1990).
- 16) H. Miyasaka, K. Morita, M. Kiri, and N. Mataga, "Ultrafast Phenomena VII," ed by C. B. Harries, E. P. Ippen, and A. H. Zewail, Springer-Verlag, Berlin (1990), p. 498.
- 17) H. Miyasaka, K. Morita, K. K. Kamada, and N. Mataga, *Bull. Chem. Soc. Jpn.*, **63**, 3385 (1990).
- 18) H. Miyasaka, K. Morita, K. Kamada, and N. Mataga, *Chem. Phys. Lett.*, **178**, 504 (1991).
- 19) H. Miyasaka, K. Morita, K. Kamada, M. Kiri, T. Nagata, and N. Mataga, *Bull. Chem. Soc. Jpn.*, **64**, 3229 (1991).
- 20) H. Miyasaka and N. Mataga, "Dynamics and Mechanism of Photoinduced Electron Transfer and Its Related Phenomena," ed by N. Mataga, T. Okada, and H. Masuhara, Elsevier, Amsterdam (1992), p. 155.
- 21) H. Miyasaka, T. Nagata, M. Kiri, and N. Mataga, *J. Phys. Chem.*, **96**, 8060 (1992).
- 22) H. Miyasaka, M. Kiri, K. Morita, N. Mataga, and Y. Tanimoto, *Chem. Phys. Lett.*, **199**, 21 (1992).
- 23) T. Kakitani, A. Yoshimori, and N. Mataga, "Electron Transfer in Inorganic, Organic and Biological Systems," ed by J. R. Bolton, N. Mataga, and G. McLenden, in "Advances in Chemistry Series 228," American Chemical Society, Washington, DC (1991), p. 45.
- 24) T. Kakitani, A. Yoshimori, and N. Mataga, *J. Phys. Chem.*, **96**, 5385 (1992).
- 25) a) T. Kakitani, N. Matsuda, T. Denda, Y. Enomoto, and N. Mataga, "Ultrafast Reaction Dynamics and Solvent Effects," ed by Y. Gauduel and P. J. Rossky, in "AIP Conference Proceedings 298," AIP Press, New York (1991), p. 395; b) N. Matsuda, T. Kakitani, T. Denda, and N. Mataga, *Chem. Phys.*, **190**, 83 (1995).
- 26) a) H. Masuhara, N. Ikeda, H. Miyasaka, and N. Mataga, *J. Spectrosc. Soc. Jpn.*, **31**, 19 (1982); b) H. Miyasaka, H. Masuhara, and N. Mataga, *Laser Chem.*, **1**, 357 (1983).
- 27) Y. Tanimoto, N. Okada, S. Takamatsu, and M. Itoh, *Bull. Chem. Soc. Jpn.*, **63**, 1342 (1990).
- 28) K. S. Peters and J. Lee, *J. Phys. Chem.*, **97**, 3761 (1993).
- 29) B. I. Greene, R. M. Hochstrasser, and R. B. Weisman, *J. Chem. Phys.*, **70**, 1247 (1979).
- 30) R. W. Anderson, "Picosecond Phenomena II," ed by R. M. Hochstrasser, W. Kaiser, and C. V. Shank, Springer, Berlin (1980), p. 163.
- 31) Y. Hirata and T. Okada, *Chem. Phys. Lett.*, **187**, 203 (1991).
- 32) H. Miyasaka, M. Hagihara, T. Okada, and N. Mataga, *Chem. Phys. Lett.*, **188**, 259 (1992).
- 33) N. Tamai, T. Asahi, and H. Masuhara, *Chem. Phys. Lett.*, **198**, 413 (1992).
- 34) M. Sisido and K. Shimada, *J. Am. Chem. Soc.*, **99**, 7785 (1977).
- 35) H. Hiratsuka, T. Yamazaki, Y. Maekawa, T. Hidaka, and Y. Mori, *J. Phys. Chem.*, **90**, 774 (1986).
- 36) G. N. Lewis and D. Lipkin, *J. Am. Chem. Soc.*, **64**,

2801 (1942).

37) a) N. Mataga, T. Okada, H. Masuhara, N. Nakashima, Y. Sakata, and S. Misumi, *J. Lumin.*, **12/13**, 159 (1976); b) T. Okada, T. Saito, N. Mataga, Y. Sakata, and S. Misumi, *Bull. Chem. Soc. Jpn.*, **50**, 331 (1977).

38) N. Mataga, M. Migita, and T. Nishimura, *J. Mol. Struct.*, **47**, 199 (1978).

39) a) T. Okada, M. Migita, N. Mataga, Y. Sakata, and S. Misumi, *J. Am. Chem. Soc.*, **103**, 4715 (1981); b) M. Migita, T. Okada, N. Mataga, Y. Sakata, S. Misumi, N. Nakashima, and K. Yoshihara, *Bull. Chem. Soc. Jpn.*, **54**, 3304 (1981).

40) N. Mataga, S. Nishikawa, T. Asahi, and T. Okada, *J. Phys. Chem.*, **94**, 1443 (1990).

41) a) N. Mataga, H. Yao, and T. Okada, *Tetrahedron*, **45**, 4683 (1989); b) H. Yao, T. Okada, and N. Mataga, *J. Phys. Chem.*, **93**, 7388 (1989).

42) T. Shida, S. Iwata, and M. Imamura, *J. Phys. Chem.*, **78**, 741 (1974).

43) R. A. Marcus, *J. Chem. Phys.*, **24**, 966 (1956).

44) a) N. Mataga, Y. Kanda, and T. Okada, *J. Phys. Chem.*, **90**, 3880 (1986); b) N. Mataga, Y. Kanda, T. Asahi,

H. Miyasaka, T. Okada, and T. Kakitani, *Chem. Phys.*, **127**, 239 (1988); c) T. Asahi and N. Mataga, *J. Phys. Chem.*, **93**, 6575 (1989); d) T. Asahi and N. Mataga, *J. Phys. Chem.*, **95**, 1956 (1991); e) T. Asahi, M. Ohkohchi, and N. Mataga, *J. Phys. Chem.*, **97**, 13132 (1993).

45) H. Miyasaka, K. Araki, and N. Mataga, to be published.

46) a) N. Mataga, T. Okada, and N. Yamamoto, *Chem. Phys. Lett.*, **1**, 119 (1967); b) N. Mataga and Y. Murata, *J. Am. Chem. Soc.*, **91**, 3114 (1969).

47) a) J. W. Verhoeven, *Pure Appl. Chem.*, **62**, 1585 (1990); b) J. W. Verhoeven, T. Scherer, and R. J. Willemse, *Pure Appl. Chem.*, **65**, 1717 (1993).

48) I. H. M. van Stokkum, T. Scherer, A. M. Brouwer, and J. W. Verhoeven, *J. Phys. Chem.*, **98**, 852 (1994).

49) F. D. Lewis, G. D. Reddy, D. D. Bassani, S. Schneider, and M. Gahr, *J. Am. Chem. Soc.*, **116**, 597 (1994), and references cited there.

50) a) Y. Hirata, Y. Kanda, and N. Mataga, *J. Phys. Chem.*, **87**, 1659 (1983); b) S. Nishikawa, T. Asahi, T. Okada, N. Mataga, and T. Kakitani, *Chem. Phys. Lett.*, **185**, 237 (1991).